Article:

Ely, J. orcid.org/0000-0003-4007-1500, Gribble, E. and Clark, C.D. (2016) The glacial geomorphology of the western cordilleran ice sheet and Ahklun ice cap, Southern Alaska. Journal of Maps, 12 (Supp 1). pp. 415-424. ISSN 1744-5647

https://doi.org/10.1080/17445647.2016.1234981

The Glacial Geomorphology of the Western Cordilleran Ice Sheet and Ahklun Ice Cap, Southern Alaska

Jeremy C. Ely *, Emily, A. Gribble and Chris D. Clark

Department of Geography, The University of Sheffield, Winter Street, Sheffield, S10 2TN, UK

*corresponding author: j.ely@sheffield.ac.uk

Abstract

During the late Wisconsinan, Southern Alaska was covered by two large ice masses; the western arm of the Cordilleran Ice Sheet and the Ahklun Mountains Ice Cap. Compared to the other ice sheets that existed during this period (e.g., the British-Irish, Laurentide and Fennoscandian ice sheets), little is known about the geomorphology they left behind. This limits our understanding of their flow pattern and retreat. Here we present systematic mapping of the glacial geomorphology of the two ice masses which existed in Southern Alaska. Due to spatially variable data availability, mapping was conducted upon digital elevation models and satellite images of varying resolutions. Offshore, we map the glacial geomorphology using available bathymetric data. For the first time, we document > 5000 subglacial lineations, recording ice flow direction. The distribution of moraines is presented, as well as features related to glacial meltwater drainage patterns (eskers and meltwater channels). Prominent troughs were also mapped on Alaska's continental shelf. This map provides the data required for a glacial inversion of these palaeo-ice masses.

1. Introduction

Approximately 70,000 km^2 (5%) of Alaska is currently glaciated (Molnia, 2008). During the late Wisconsinan (~30 to 10 kya) ice extent was approximately 10 times greater than this, with previous glaciations greater still in extent (Kaufman and Manley, 2004; Kaufman et al., 2011). The majority of this ice was contained within three ice masses; an ice cap over the Brooks range to the north of Alaska (Hamilton and Porter, 1975), a second ice cap over the Ahklun Mountains (Briner and Kaufman, 2000) and a much larger ice sheet in the south. The latter formed the Western edge of the Cordilleran ice sheet at its maximum (Booth et al., 2004) and covered the Aleutian Islands in the West, the Alaskan Peninsula and the Wrangell Mountains in the East (Mann and Peteet, 1994; Kaufman et al., 2011). As well as containing a large volume of fresh water, these Alaskan ice masses may have formed a barrier to human migration across the land bridge, known as Beringia, which existed between Alaska and Russia during the last glacial period (Mandryk et al., 2001; Misarti et al., 2012). Figure 1 shows the proposed extent of ice at different times across southern Alaska. This paper focuses upon the geomorphology left behind by the two principle ice masses in this area; the Ahklun Mountains Ice Cap and the Western Cordilleran Ice Sheet (Figure 1).

The maximum extent of the Alaskan ice masses has been proposed and mapped (e.g., Figure 1, Kaufman and Manley, 2004; Kaufman et al., 2011), but less is known about the pattern of the retreat of these ice masses. This is partially due to a lack of a map of the glacial landforms which this ice sheet left behind. The distribution of moraines, meltwater channels, glacial troughs, eskers and subglacial bedforms can be used to reconstruct ice sheets via a glacial inversion method (e.g., Kleman and Borgström, 1996, Clark, 1999; Stokes et al., 2015). This technique has proven informative for the British-Irish (e.g., Greenwood and Clark, 2008; Hughes et al., 2010; Clark et al., 2012), Fennoscandian (e.g., Kleman et al., 1997; Stroeven et al., 2015), Cordilleran (e.g., Margold et al., 2013) and Laurentide ice sheets (e.g., Boulton and Clark, 1990b; Trommelen et al., 2014). Here we present mapping of the glacial geomorphology for the Ahklun Mountains Ice Cap and the Western Cordilleran Ice Sheet across the area they each encompassed during the late Wisconsinan. This map will form the basis of an empirical reconstruction of these ice masses.

2. Methods

Onshore, glacial landforms were identified and mapped using three sources of data. All onshore sources were obtained from the USGS website (www.earthexplorer.usgs.gov). The datasets used and their resolution are listed in Table 1. A digital elevation model (DEM) derived from interferometric synthetic aperture radar (IfSAR) provided the highest resolution data (5 m), but is not available across the whole of Alaska (Figure 2). Below 60^{o}N the shuttle radar topography mission DEM (SRTM; 30 m resolution) was used (Figure 2). To fill the space where neither of these two datasets were available, glacial landforms were identified on Landsat ETM+ imagery (15 m pan-chromatic resolution), which is available globally. Offshore, elevation models are available from NOAA (https://maps.ngdc.noaa.gov/viewers/bathymetry/). DEMs of various resolutions were available (Table 1). Where high resolution bathymetric data was not available, a coarser resolution (500 m) elevation model was used. Only the largest glacial features such as glacial troughs or large moraines (several km’s in length and 10’s of m in amplitude) were visible on this DEM.

To maximise landform identification, we adopted a repeat pass approach to mapping, checking each area multiple times. However, our mapping is necessarily limited where high resolution offshore elevation models are unavailable. Where high resolution data was available, for example the IfSAR DEM (Table 1 and Figure 2), this enabled a high level of identification and subsequent mapping of landforms. As a consequence, these areas are mapped in more detail than others. Therefore, we anticipate more detailed geomorphology may be revealed as higher resolution datasets become available, prompting future work. Landform preservation, burial and submergence also limit landform identification.

Glacial landforms were identified on hill-shaded relief models created from the available DEMs. Two hill-shades were created from each DEM, illuminating from 45^{o} and 315^{o} to avoid azimuth biasing (Smith and Clark, 2005; Figure 3A and B). Hill-shades were made semi-transparent and overlaid on a DEM in order to avoid mapping hollows. False colour composite (bands 4, 3 and 2) Landsat images were enhanced using local image statistics in order to highlight subtle topography (e.g. Ely and Clark, 2016). The pan-chromatic band was used to further refine the imagery, to give a horizontal resolution of 15 m (Figure 3C). Features were mapped using a combination of hill-shade illumination angles and satellite data (Figure 3D).

The following features were identified and mapped: subglacial lineations, streamlined bedrock, moraines, eskers, meltwater channels and glacial troughs. Subglacial lineations were mapped as polygons around their break of slope. Break of slope was identifiable on hill-shaded DEMs (Hughes et al., 2010; Hiller et al., 2015; Figure 3 A and B). On satellite imagery these breaks of slope were visible as changes in reflection or vegetation (Spagnolo et al., 2014). On the higher resolution IfSAR DEM (Table 1), many streamlined features were qualitatively different in appearance, giving the impression that they were predominately composed of bedrock (e.g., Bradwell, 2005; Lane et al., 2015; Figure 4). Differentiation of these features was aided by a surface geology map. Where possible, moraines were also mapped as polygons. Often, moraines were composed of several ridges comprising a moraine complex. Where this was the case, the smaller ridges were mapped as polylines and the moraine complex as a polygon (Figure 5). Furthermore, some smaller moraines were mapped solely as polylines along their crest. Eskers were also mapped as polylines along their crestline. Glacial meltwater channels were mapped as polygons along their thalweg. These were identified as glacial in origin due to their discordance with modern day fluvial drainage patterns (c.f. Greenwood et al., 2007). However, it is reasonable to expect that a channel may have been occupied by both a glacially dominated source of water and by a fluvial or glaciofluvial water source at a later stage. Finally, glacial troughs were mapped as polylines along their banks, using 3D profiles and hill-shading to define their edges (Spagnolo and Clark, 2009). Unlike other ice sheets (e.g., Hättestrand and Kleman, 1999; Trommelen and Ross, 2010; McHenry and Dunlop, 2015), no examples of subglacial ribs, which form transverse to flow direction, were noted.

3. Map description

The Main Map was produced in ArcGIS 10.1. It is comprised of 12,846 digitised polylines and polygons. The background for the map is a merged bathymetric and terrestrial elevation model downloaded from the National Oceanic and Atmospheric Administration (NOAA, www.ngdc.noaa.gov). The extent of modern day glaciers, available from the Randolph Glacier Inventory (version 5, www.glims.org/RGI/), is also included on the map in order to contrast with landforms created by more extensive glaciers. The map is projected in NAD 1983 CORS96 Alaska Albers and is designed to be printed on 2A0 paper, at a scale of 1:1,000,000. The distribution, frequency and characteristics of the mapped glacial landforms are discussed below.

3.1. Subglacial lineations and streamlined bedrock

Despite their frequency both in the literature and upon previously glaciated landscapes, the subglacial bedforms of Alaska have hitherto received little to no mention within the literature. Here, 5878 subglacial lineations, which are formed aligned with flow direction, were mapped from the 4 main sources of data (Table 2). Exemplars were found near Becharof Lake (Figure 3), within McCarthy Borough, Valdez-Cordova (Figure 6A) and at the confluence between the West and East Forks of the Yetna River (Figure 6B). Lineations were also observed in the Akhlun ice cap area (Main Map; Figure 6C), where they record a radial flow pattern outward from the centre of the mountain range and along valley floors. Furthermore, subglacial lineations were also observed on offshore bathymetry (Figure 6D).

Subglacial lineations form a morphological continuum of landforms spanning those typically referred to as drumlins, to mega-scale glacial lineations (Ely et al., 2016). The majority of Alaskan subglacial lineations would fall into the shorter end of this continuum, having low length-width ratios and thus conforming to the part of this continuum which is typically referred to as drumlins (Clark et al., 2009). However, a few drumlins are remarkably long, elongate and parallel, reaching lengths above 6 km, exceeding the size of bedforms typically found on ice stream beds (e.g., Figure 6B; Spagnolo et al., 2014). Future work is required to establish the potential role of palaeo-ice streaming across Alaska.

Additionally, 1239 examples of subglacially streamlined bedrock landforms were mapped (Table 1). These are typically 500 m long and a few metres high: exemplars are shown on Figure 4. These landforms can also be used to infer past flow direction and possible ice streaming (e.g., Bradwell et al., 2008; Lane et al., 2015), but likely form by a separate set of processes to other subglacial bedforms (Dionne, 1987), hence their separation on our map. Streamlined bedrock is especially prominent on the mountains to the west of the Copper Basin (Figure 4). This suggests that at some point the Cordilleran Ice Sheet covered these mountains.

3.2. Moraines

Moraines were mapped as polylines and polygons (n = 4101) from the different data sources (Table 3). A large range of moraine sizes were observed, the smallest being less than a metre high and a few metres wide, with the larger moraine complexes several tens of metres in height and kilometres wide. Some of the most impressive morainic patterns were found on the northern sides of the Alaskan Peninsula (Figure 7A), the Aleutian Range (Figure 7B) and the Alaska Range (Figure 7C). Impressive moraines were also noted to emanate from the Akhlun mountains (Figures 5 and 7D). Comparatively few moraines were noted offshore, at least partially due to sparse data coverage or burial by post-glacial sediment. Many of the moraines form concentric, looped patterns (Figures 5 and 7) suggesting along valley margin standstills as the ice retreated.

3.3. Eskers and meltwater channels

Eskers were only observed on the IfSAR DEM, either due to the higher resolution of this data, or perhaps eskers were only formed in the region that this DEM covers (Figure 2). Polylines (n = 592) included on the Main Map represent individual esker segments (e.g., Storrar et al., 2014), the shortest of which were a few tens of metres in length, but in places were traced for over 4 km. Compared to the Laurentide (Storrar et al., 2014) and Fennoscandian ice sheets (Stroven et al., 2015) eskers are rare. This perhaps highlights differences in the drainage of these ice sheets, or points toward a poor preservation of eskers in Alaska. An example esker is shown in Figure 8A. As has been reported for other palaeo-ice sheets (Greenwood et al., 2016), eskers were observed to switch into meltwater channels (e.g., Figure 8B), but meltwater channels were also observed in isolation from eskers (e.g., Figure 8C). In total, 1979 meltwater channels were mapped, again ranging from a few tens of metres to several kilometres in length. Future work is required to classify these meltwater channels before they can be used for glacial inversion (e.g., Greenwood et al., 2007).

3.4. Troughs

Polylines (n= 135) marking the edge of troughs are included on the Main Map. The troughs are typically 50 to 300 m deep, and several hundreds of metres wide. The largest trough forms the Shelikof Strait, between the Aleutian Mountains and Kodiak Island, through which ice has been hypothesised to flow (Mann and Peteet, 1994). Further troughs are evident across the southern Alaskan continental shelf (Figure 9C and D; Schwartz et al., 2015). Elsewhere, ice streams form along such troughs (e.g., the Norwegian channel ice stream (Sejrup et al., 2003) and the Lambert Glacier-Amery ice shelf system (Hambrey and Dowdeswell, 1994)). However, a lack of high resolution bathymetry within the Shelikof Strait, and other troughs, prohibits any recognition of a possible palaeo-ice stream imprint (Stokes and Clark, 1999).

4. Summary and Conclusions

The Cordilleran Ice Sheet and Ahklun Mountains Ice Cap left behind a wealth of geomorphological evidence during the late Wisconsinan in southern Alaska. Here we present the first systematic map of the glacial geomorphology across the areas formally occupied by these ice masses. Our mapping covers the terrestrial portion of these ice sheets, and, where bathymetric data exists, the submerged geomorphology. The map documents numerous subglacial lineations, which may represent the tracks of palaeo-ice streams. Large, looping moraine sequences record the recession of the ice masses. We also note features related to glacial meltwater, channels and eskers, as well as systems of glacial troughs offshore. This map provides the basis for a future empirical reconstruction of the ice masses in this area.

5. Software

Mapping and data manipulation were conducted in ESRI ArcGIS 10.1.

6. Acknowledgements

This work was funded by a Sheffield University Research Experience (S.U.R.E) grant. We would like to thank Danni Pearce, Martin von Wyss, Jakob Heyman, Giedrė Beconytė, Martin Margold and the editors for their useful comments.

Map Design

The Main Map was produced using ArcMap v 10.1. The names of significant mountain ranges, river basins and oceans are included in order to orientate the map user. The background to the map is a semi-transparent DEM, classified to highlight the break of the continental shelf and to show upland regions. Modern day glacier distribution is shown to explain "blank" areas on the map where landforms are masked by ice, and to provide a contrast with the more extensive geomorphology left behind by the last ice sheets in Alaska.

7. References

Booth, D.B., Troost, K.G., Clague, J.J. and Waitt, R.B., 2004. The Cordilleran ice sheet. The Quaternary Period in the United States, 1, pp.17-43.

Boulton, G.S. and Clark, C.D., 1990. The Laurentide ice sheet through the last glacial cycle: the topology of drift lineations as a key to the dynamic behaviour of former ice sheets. Transactions of the Royal Society of Edinburgh: Earth Sciences, 81(04), pp.327-347.

Bradwell, T., 2005. Bedrock megagrooves in Assynt, NW Scotland.Geomorphology, 65(3), pp.195-204.

Bradwell, T., Stoker, M. and Krabbendam, M., 2008. Megagrooves and streamlined bedrock in NW Scotland: the role of ice streams in landscape evolution. Geomorphology, 97(1), pp.135-156.

Briner, J.P. and Kaufman, D.S., 2000. Late Pleistocene glaciation of the southwestern Ahklun mountains, Alaska. Quaternary Research, 53(1), pp.13-22.

Clark, C.D., 1999. Glaciodynamic context of subglacial bedform generation and preservation. Annals of Glaciology, 28(1), pp.23-32.

Clark, C.D., Hughes, A.L., Greenwood, S.L., Spagnolo, M. and Ng, F.S., 2009. Size and shape characteristics of drumlins, derived from a large sample, and associated scaling laws. Quaternary Science Reviews, 28(7), pp.677-692.

Clark, C.D., Hughes, A.L., Greenwood, S.L., Jordan, C. and Sejrup, H.P., 2012. Pattern and timing of retreat of the last British-Irish Ice Sheet.Quaternary Science Reviews, 44, pp.112-146.

Dionne, J.C., 1987. Tadpole rock (rocdrumlin): a glacial streamline moulded form. In Drumlin Symposium. Rotterdam: Balkema (Vol. 149, p. 159).

Ely, J.C. and Clark, C.D., 2016. Flow-stripes and foliations of the Antarctic ice sheet. Journal of Maps, 12(2), pp.249-259.

Ely, J.C., Clark, C.D., Spagnolo, M., Stokes, C.R., Greenwood, S.L., Hughes, A.L., Dunlop, P. and Hess, D., 2016. Do subglacial bedforms comprise a size and shape continuum?. Geomorphology, 257, pp.108-119.

Greenwood, S.L., Clark, C.D. and Hughes, A.L., 2007. Formalising an inversion methodology for reconstructing ice-sheet retreat patterns from meltwater channels: application to the British Ice Sheet. Journal of Quaternary Science, 22(6), pp.637-645.

Greenwood, S.L. and Clark, C.D., 2008. Subglacial bedforms of the Irish ice sheet. Journal of Maps, 4(1), pp.332-357.

Greenwood, S.L., Clason, C.C., Helanow, C. and Margold, M., 2016. Theoretical, contemporary observational and palaeo-perspectives on ice sheet hydrology: Processes and products. Earth-Science Reviews, 155, pp.1-27.

Hambrey, M.J. and Dowdeswell, J.A., 1994. Flow regime of the Lambert Glacier-Amery Ice Shelf system, Antarctica: structural evidence from Landsat imagery. Annals of Glaciology, 20(1), pp.401-406.

Hamilton, T.D. and Porter, S.C., 1975. Itkillik glaciation in the Brooks Range, northern Alaska. Quaternary Research, 5(4), pp.471-497.

Hättestrand, C. and Kleman, J., 1999. Ribbed moraine formation. Quaternary Science Reviews, 18(1), pp.43-61.

Hillier, J.K., Smith, M.J., Armugam, R., Barr, I., Boston, C.M., Clark, C.D., Ely, J., Frankl, A., Greenwood, S.L., Gosselin, L. and Hättestrand, C., 2015. Manual mapping of drumlins in synthetic landscapes to assess operator effectiveness. Journal of Maps, 11(5), pp.719-729.

Hughes, A.L., Clark, C.D. and Jordan, C.J., 2010. Subglacial bedforms of the last British Ice Sheet. Journal of Maps, 6(1), pp.543-563.

Kaufman, D.S., Manley, W.F., 2004. Pleistocene maximum and Late Wisconsin glacier extents across Alaska, USA. In: Ehlers, J., Gibbard, P.L. (Eds.), Quaternary Glaciations—Extent and Chronology, Part II: North America. Developments in Quaternary Science, vol. 2 Elsevier, Amsterdam, pp. 9–27.

Kaufman, D.S., Young, N.E., Briner, J.P. and Manley, W.F., Alaska Palaeo-Glacier Atlas (Version 2). In: Ehlers, J., Gibbard, P.L. and Hughes, P.D. Quaternary Glaciations – Extent and Chronology. Developments in Quaternary Science, vol. 2, Elsevier, Amsterdam, pp. 427-445.

Kleman, J. and Borgström, I., 1996. Reconstruction of palaeo-ice sheets: the use of geomorphological data. Earth surface processes and landforms,21(10), pp.893-909.

Kleman, J., Hättestrand, C., Borgström, I. and Stroeven, A., 1997. Fennoscandian palaeoglaciology reconstructed using a glacial geological inversion model. Journal of glaciology, 43(144), pp.283-299.

Lane, T.P., Roberts, D.H., Rea, B.R., Cofaigh, C.Ó. and Vieli, A., 2015. Controls on bedrock bedform development beneath the Uummannaq Ice Stream onset zone, West Greenland. Geomorphology, 231, pp.301-313.

Mandryk, C.A., Josenhans, H., Fedje, D.W. and Mathewes, R.W., 2001. Late Quaternary paleoenvironments of Northwestern North America: implications for inland versus coastal migration routes. Quaternary Science Reviews, 20(1), pp.301-314.

Mann, D.H. and Peteet, D.M., 1994. Extent and timing of the last glacial maximum in southwestern Alaska. Quaternary Research, 42(2), pp.136-148.

Margold, M., Jansson, K.N., Kleman, J., Stroeven, A.P. and Clague, J.J., 2013. Retreat pattern of the Cordilleran Ice Sheet in central British Columbia at the end of the last glaciation reconstructed from glacial meltwater landforms. Boreas, 42(4), pp.830-847.

McHenry, M. and Dunlop, P., 2015. The subglacial imprint of the last Newfoundland Ice Sheet, Canada. Journal of Maps.

Misarti, N., Finney, B.P., Jordan, J.W., Maschner, H.D., Addison, J.A., Shapley, M.D., Krumhardt, A. and Beget, J.E., 2012. Early retreat of the Alaska Peninsula Glacier Complex and the implications for coastal migrations of First Americans. Quaternary Science Reviews, 48, pp.1-6.

Molnia, B.F., 2008. Glaciers of Alaska. US Geological Survey professional paper, (1386K).

Sejrup, H.P., Larsen, E., Haflidason, H., Berstad, I.M., Hjelstuen, B.O., Jonsdottir, H.E., King, E.L., Landvik, J., Longva, O., Nygård, A. and Ottesen, D., 2003. Configuration, history and impact of the Norwegian Channel Ice Stream. Boreas, 32(1), pp.18-36.

Smith, M.J. and Clark, C.D., 2005. Methods for the visualization of digital elevation models for landform mapping. Earth Surface Processes and Landforms, 30(7), pp.885-900.

Spagnolo, M. and Clark, C.D., 2009. A geomorphological overview of glacial landforms on the Icelandic continental shelf. Journal of Maps, 5(1), pp.37-52.

Spagnolo, M., Clark, C.D., Ely, J.C., Stokes, C.R., Anderson, J.B., Andreassen, K., Graham, A.G. and King, E.C., 2014. Size, shape and spatial arrangement of mega-scale glacial lineations from a large and diverse dataset. Earth Surface Processes and Landforms, 39(11), pp.1432-1448.

Stokes, C.R. and Clark, C.D., 1999. Geomorphological criteria for identifying Pleistocene ice streams. Annals of Glaciology, 28(1), pp.67-74.

Stokes, C.R., Tarasov, L., Blomdin, R., Cronin, T.M., Fisher, T.G., Gyllencreutz, R., Hättestrand, C., Heyman, J., Hindmarsh, R.C., Hughes, A.L. and Jakobsson, M., 2015. On the reconstruction of palaeo-ice sheets: Recent advances and future challenges. Quaternary Science Reviews, 125, pp.15-49.

Storrar, R.D., Stokes, C.R. and Evans, D.J., 2014. Morphometry and pattern of a large sample (> 20,000) of Canadian eskers and implications for subglacial drainage beneath ice sheets. Quaternary Science Reviews, 105, pp.1-25.

Stroeven, A.P., Hättestrand, C., Kleman, J., Heyman, J., Fabel, D., Fredin, O., Goodfellow, B.W., Harbor, J.M., Jansen, J.D., Olsen, L. and Caffee, M.W., 2015. Deglaciation of Fennoscandia. Quaternary Science Reviews.

Trommelen, M. and Ross, M., 2010. Subglacial landforms in northern Manitoba, Canada, based on remote sensing data. Journal of Maps, 6(1), pp.618-638.

Trommelen, M.S., Ross, M. and Ismail, A., 2014. Ribbed moraines in northern Manitoba, Canada: characteristics and preservation as part of a subglacial bed mosaic near the core regions of ice sheets. Quaternary Science Reviews, 87, pp.135-155.

Table 1 – Resolution and source of datasets used

Dataset	Horizontal Resolution (m)	Source
Merged on and offshore DEM	500	NOAA
SRTM DEM	30	Earthexplorer.usgs.gov
Landsat ETM+	15 pan-chromatic	Earthexplorer.usgs.gov
IfSAR DEM	5	Earthexplorer.usgs.gov
Adak Bathymetry	30	NOAA
Akutan Bathymetry	12 – 200	NOAA
Chignik Bathymetry	10 - 30	NOAA
Chenega Bathymetry	12	NOAA
Coldbay Bathymetry	12 – 200	NOAA
Cordova Bathymetry	10 – 90	NOAA
Dutch Harbour Bathymetry	15	NOAA
Homer Bathymetry	12 – 200	NOAA
Kachemak Bay Bathymetry	4	NOAA
Kingcove Bathymetry	12 – 200	NOAA
Kodiak Bathymetry	12 – 200	NOAA
Nikolski Bathymetry	30	NOAA
Prince William Sound Bathymetry	4 – 200	NOAA
Sand Point Bathymetry	90	NOAA
Seldovia Bathymetry	30 – 90	NOAA
Seward Bathymetry	4 – 200	NOAA
Tatilek Bathymetry	8	NOAA
Yakutat Bathymery	4 – 200	NOAA

Table 2. Number of subglacial lineations and streamlined bedrock features per dataset.

Landform type	**Data source**	**Number of landforms**
Subglacial lineations	Landsat ETM+	541
	IfSAR DEM	3150
	SRTM DEM	1749
	Offshore Bathymetry	460
Streamlined bedrock	IfSAR DEM	1239

Table 3. The number of mapped moraines per data set.

Data source	**Number of moraine features**
Landsat ETM+	514
IfSAR DEM	949
SRTM DEM	1135
Offshore Bathymetry	403

Figure Captions:

Figure 1. Overview of the principle palaeo-ice masses in South Alaska. Glacial limits from Alaska Paleo-Glacier Atlas, Version 2 (proposed by Kaufman et al. (2011) and updated from Kaufman and Manley, (2004); www.ncdc.noaa.gov/paleo/alaska-glacier.html). Numbers and boxes show locations of subsequent figures.

Figure 2. Distribution of datasets used. Coastlines from thematicmapping.org

Figure 3. Subglacial lineations (drumlins) near Becharof Lake. (A) SRTM hill-shaded DEM, illuminated from the NW. Arrow denotes approximate palaeo-ice flow direction. (B) SRTM hill-shaded DEM, this time illuminated from the NE. (C) Landsat false colour composite of the same drumlins. (D) Mapped subglacial lineation outlines.

Figure 4. Examples of glacially streamlined bedrock. Arrows denote approximate palaeo-ice flow direction. (A) Hill-shaded IfSAR DEM of bedrock lineations West of Talkeetna, Matanuska-Susitna Borough. (B) Hill-shaded IfSAR DEM of a mixture of streamlined bedrock, crag and tails, and sediment lineations, near McKinley Fall, Matanuska-Susitna Borough. Regions of bedrock highs correspond to subglacial lineations with a qualitatively different morphology, thought to be streamlined bedrock.

Figure 5. Examples of moraine mapping. (A) Hill-shaded SRTM DEM of prominent moraines of both the Cordilleran Ice Sheet and the Akhlun Mountains Ice Cap. (B) Derived mapping. Note

how the areas of looping moraines denoted by polygons also have prominent ridges mapped as polylines. Kvichak Bay begins to the south east of these images.

Figure 6. Examples of Alaskan subglacial lineations. Arrows denote palaeo-ice flow direction. (A) Lineations within McCarthy Borough, dissected by the Chitina River. (B) Elongate lineations near the confluence between the West and East Forks of the Yetna River. (C) Hill-shaded STRM DEM of subglacial lineations (drumlins) on the valley floors of the Akhlun ice cap. This example depicts the area near lakes Nerka, Aleknagik and Nunavaugaluk. (D) Hill-shaded bathymetry of submerged subglacial lineations, SE of Mitrofania Bay.

Figure 7. Examples of Alaskan moraines. Arrows denote palaeo-ice flow direction and terminate at the moraines. (A) Hill-shaded SRTM DEM of moraines at the heads of Morzhovoi Bay (left) and Cold Bay (east). (B) Hill-shaded SRTM DEM of moraines north of the Alleutians, north of Mother Goose lake. (C) Hill-shaded SRTM DEM of concentric looped moraines, related to the Akhlun ice cap, east of Tikchik Lake. (D) Hill-shaded IfSAR DEM of moraines north of Mt. Denali.

Figure 8. Examples of eskers and meltwater channels on hill-shaded IfSAR DEMs. (A) A large esker, passing through Lower Tangle Lake, Paxson. (B) An esker which grades into a meltwater channel, west of Dickey Lake, Valdez-Cordova. (C) A series of meltwater channels, located along the Denali Highway, east of Alpine Creek Lodge.

Figure 9. Examples and profiles across glacially occupied troughs. Images are hill-shaded merged bathymetry and elevation data. (A) The Shelikof Strait. (B) Troughs and fjords, south of Kenai Fjords National Park. (C) Profiles across lines Y to Y' and Z to Z', located on (A) and (B).

Figures

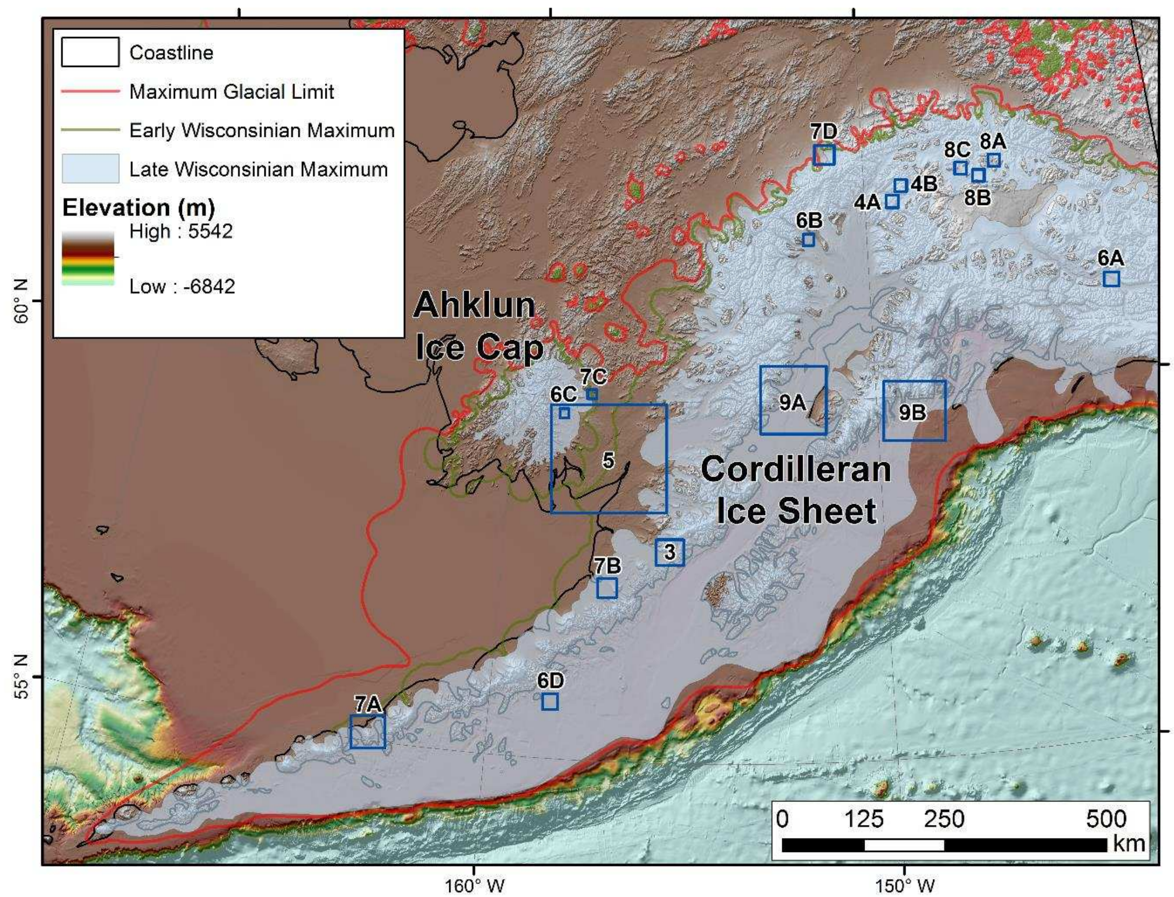

Figure 1

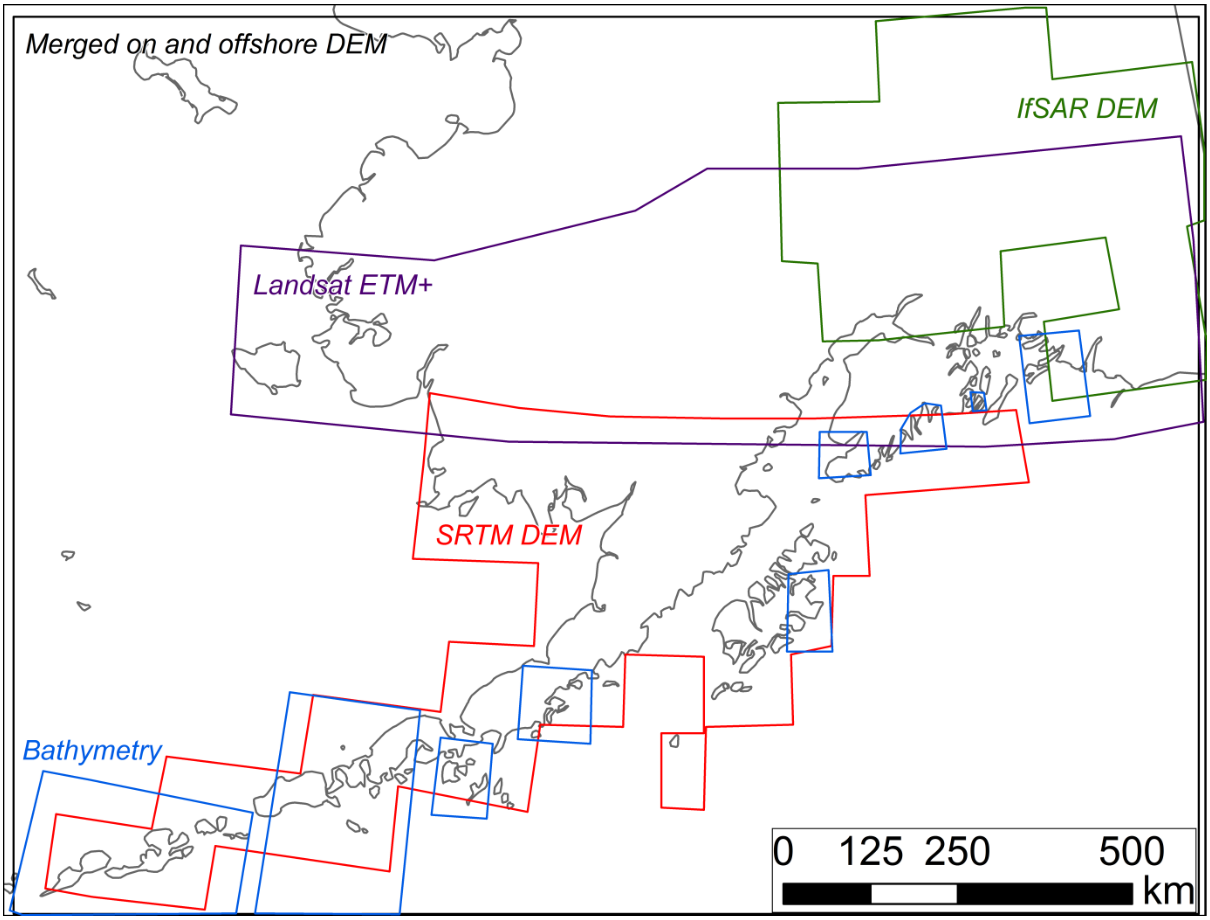
Merged on and offshore DEM
IfSAR DEM
Landsat ETM+
SRTM DEM
Bathymetry
0
125
250
500
km

Figure 2

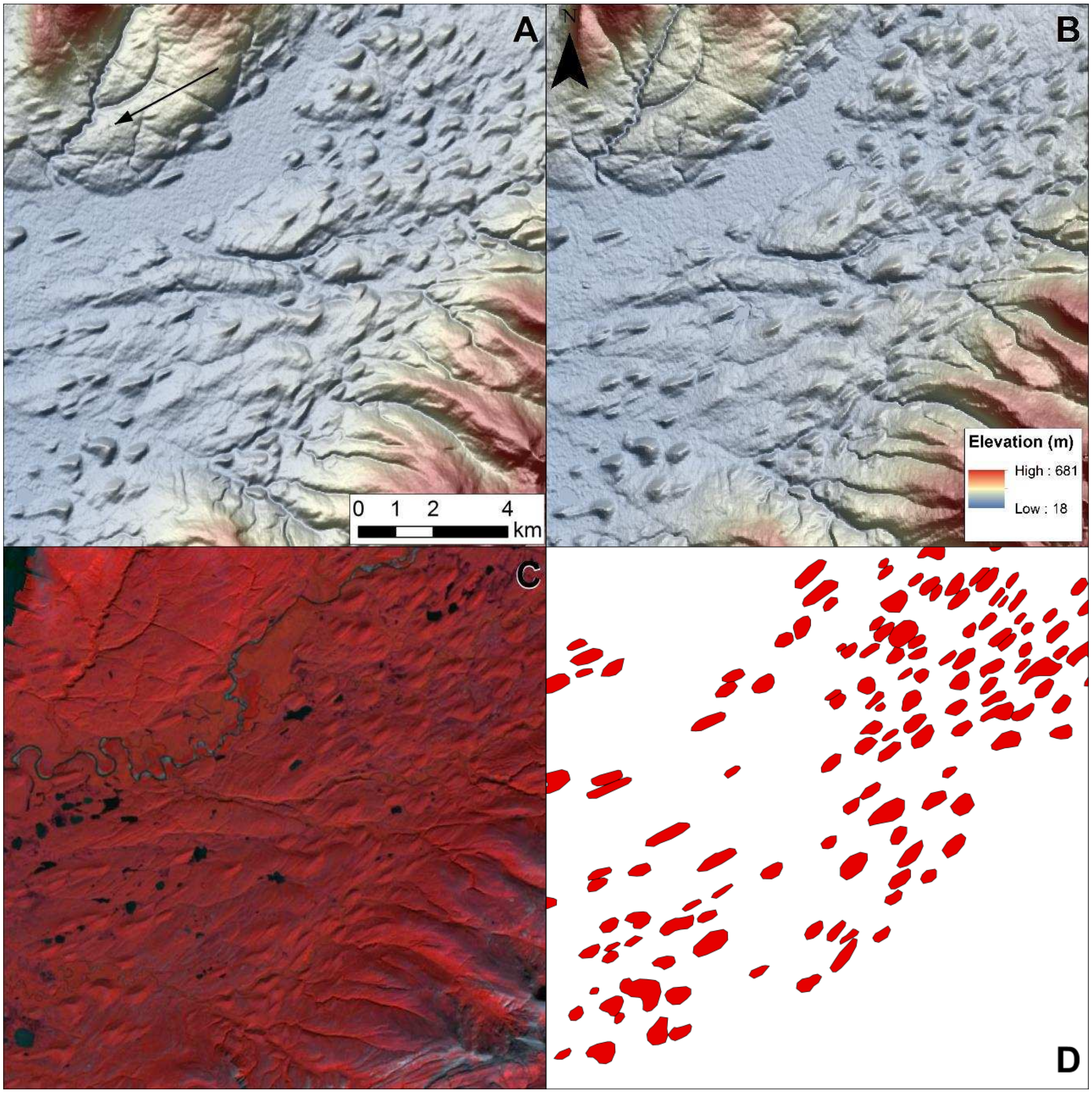

Figure 3

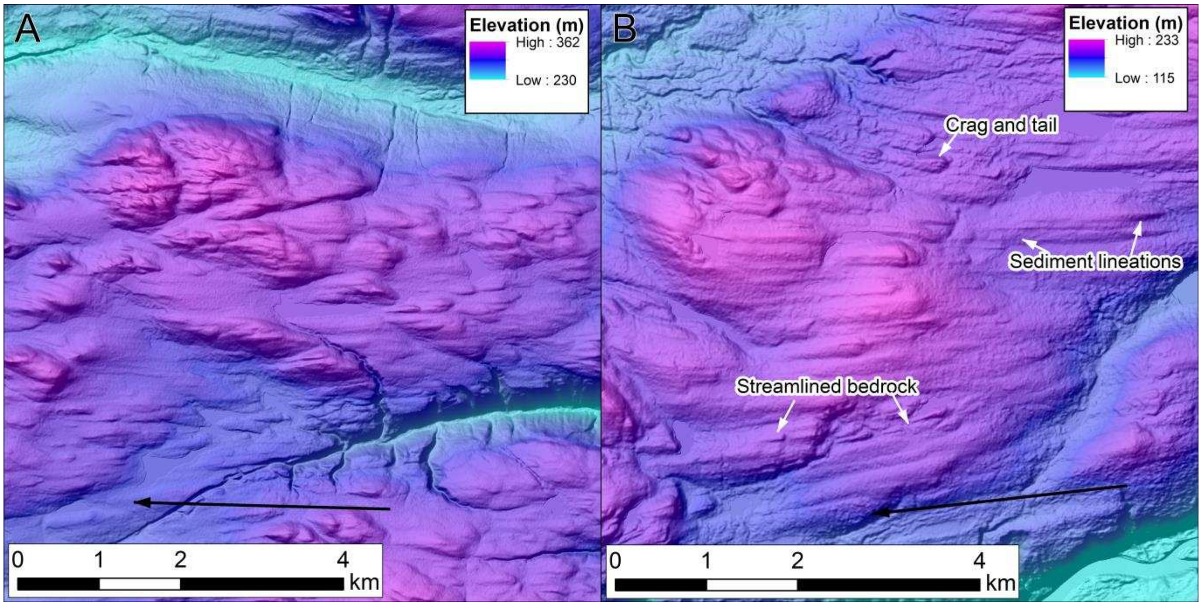
A
Elevation (m)
High : 362
Low : 230
0 1 2 4 km
B
Elevation (m)
High : 233
Low : 115
Crag and tail
Sediment lineations
Streamlined bedrock
0 1 2 4 km

Figure 4

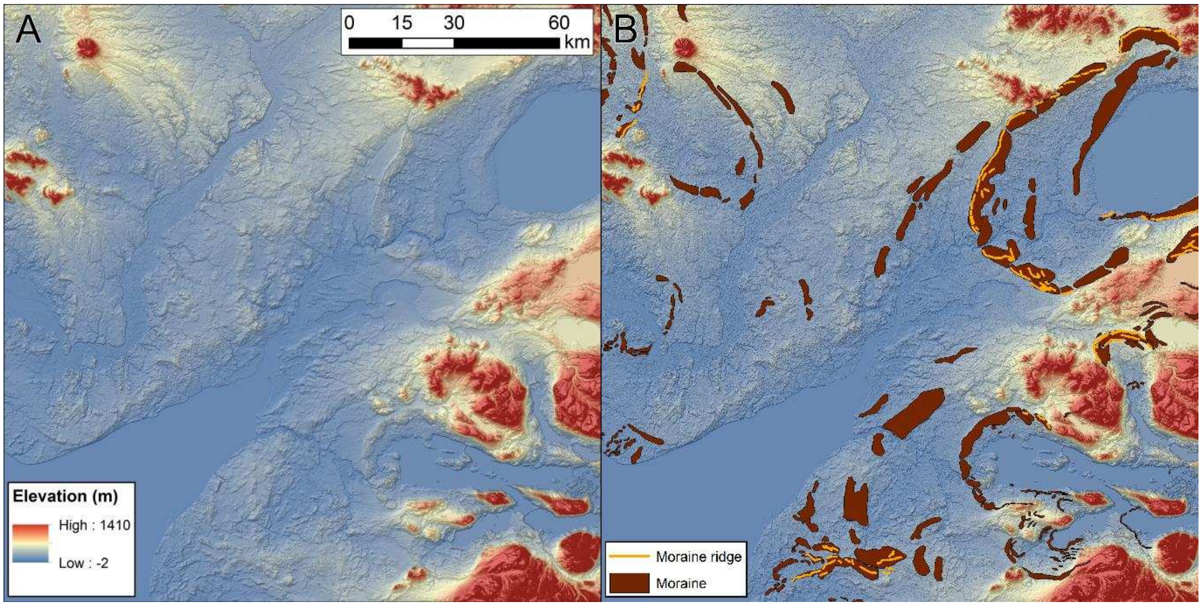
A
B
0 15 30 60
km
Elevation (m)
High : 1410
Low : -2
Moraine ridge
Moraine

Figure 5

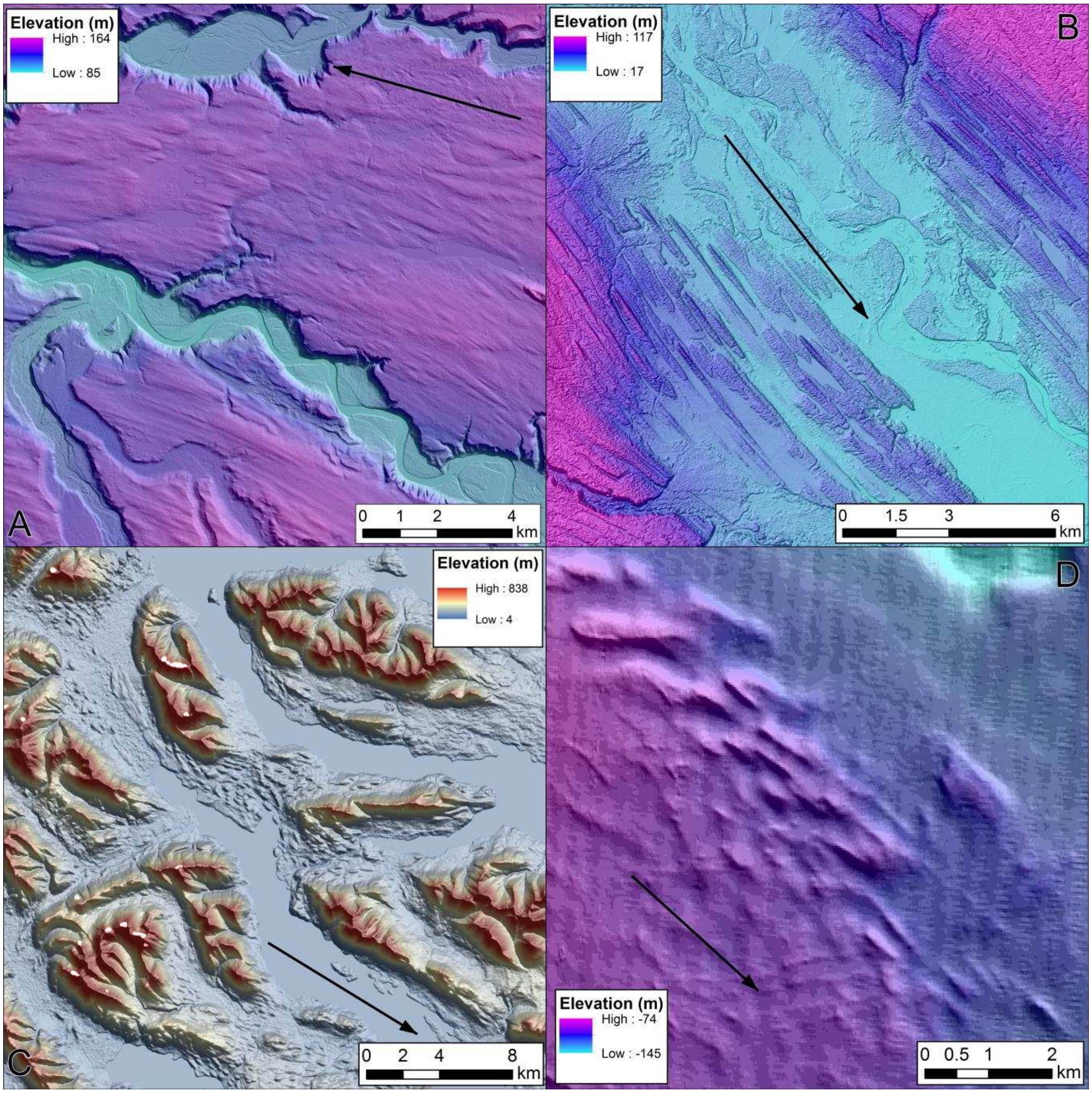
Elevation (m)
High : 164
Low : 85
0 1 2 4 km
A
Elevation (m)
High : 117
Low : 17
B
0 1.5 3 6 km
Elevation (m)
High : 838
Low : 4
0 2 4 8 km
C
Elevation (m)
High : -74
Low : -145
D
0 0.5 1 2 km

Figure 6

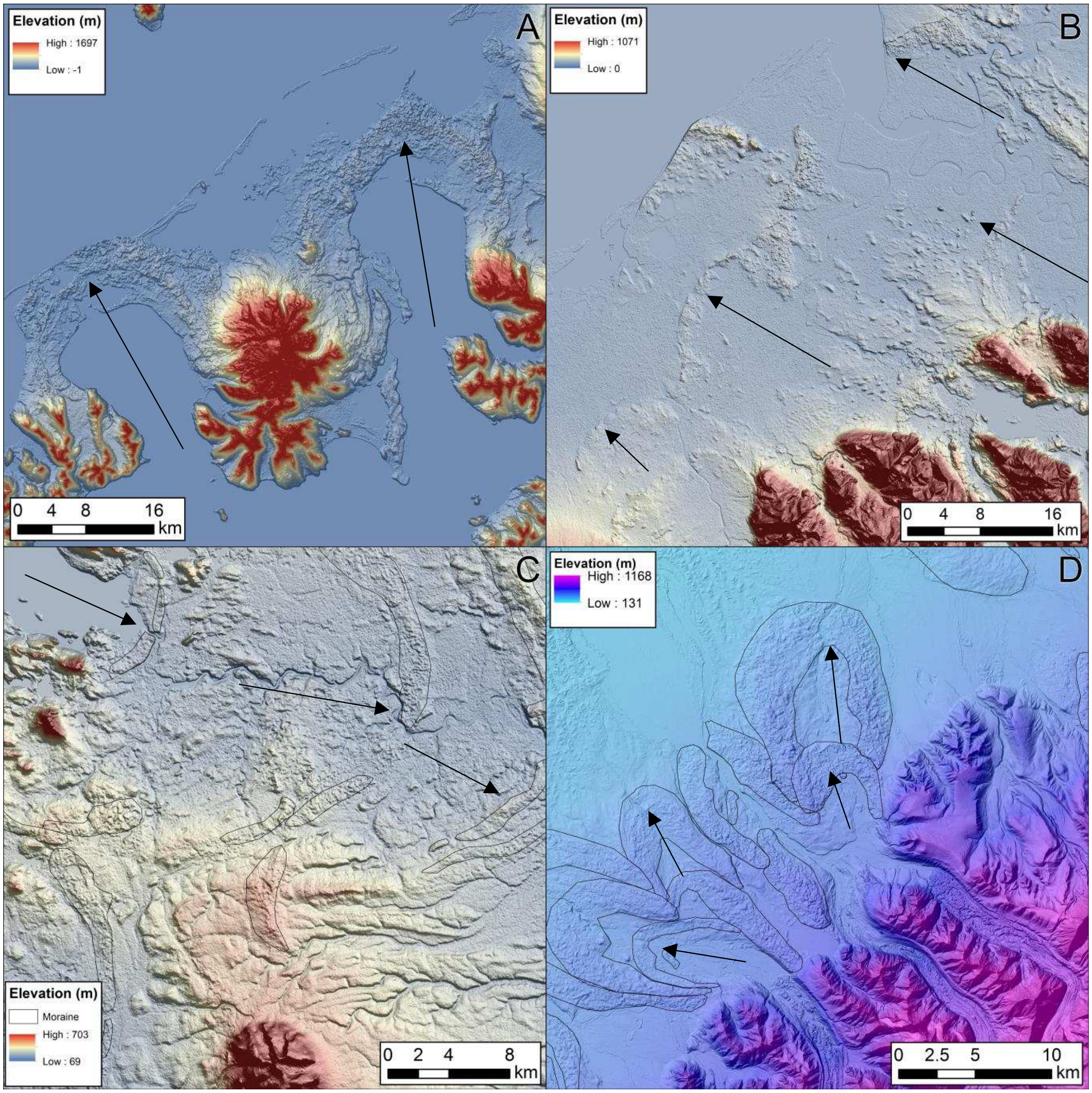
A
Elevation (m)
High : 1697
Low : -1
0 4 8 16
km
B
Elevation (m)
High : 1071
Low : 0
0 4 8 16
km
C
Elevation (m)
Moraine
High : 703
Low : 69
0 2 4 8
km
D
Elevation (m)
High : 1168
Low : 131
0 2.5 5 10
km

Figure 7

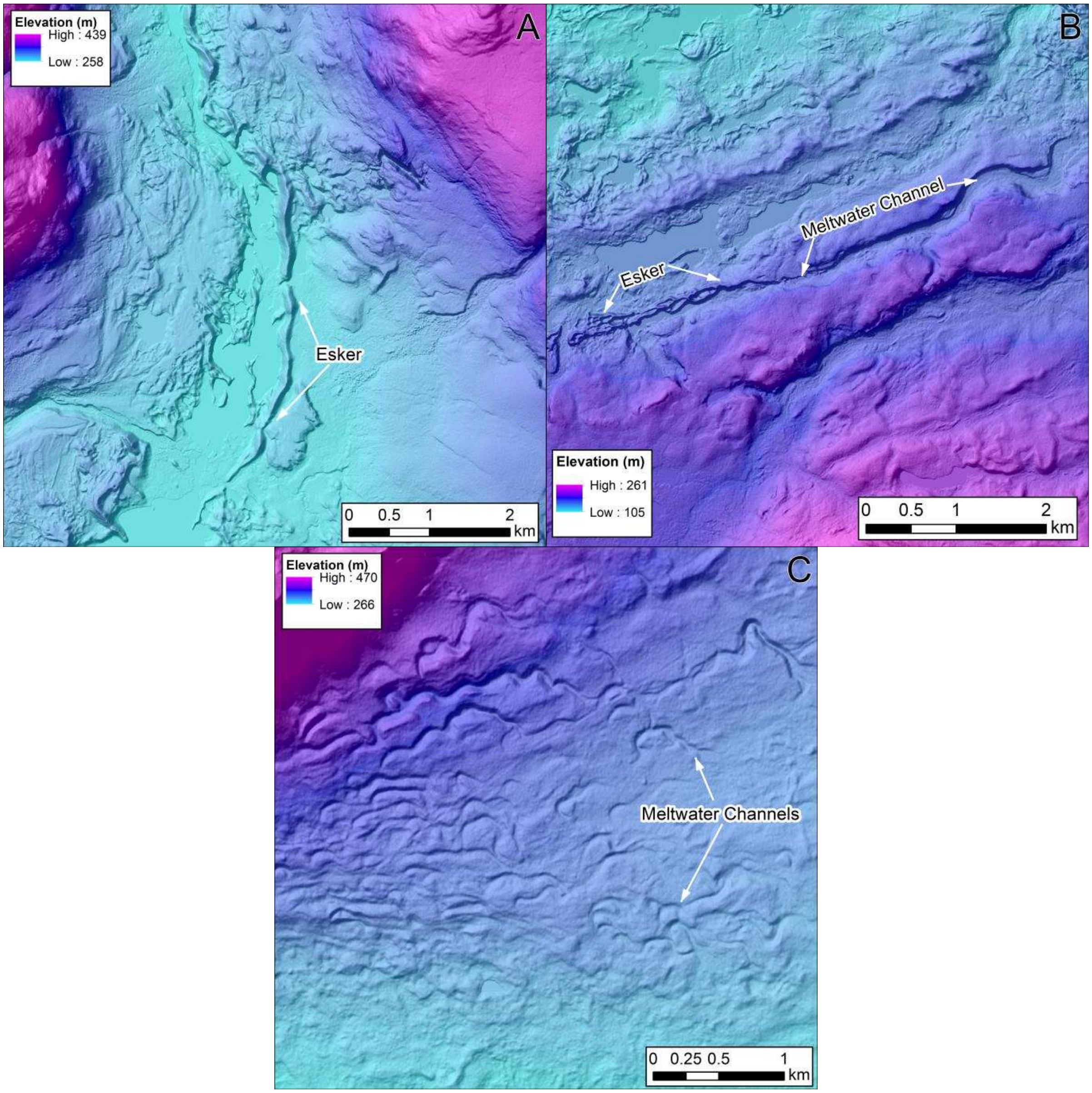

Elevation (m)
High : 439
Low : 258
A
Esker
0 0.5 1 2
km
B
Meltwater Channel
Esker
Elevation (m)
High : 261
Low : 105
0 0.5 1 2
km
Elevation (m)
High : 470
Low : 266
C
Meltwater Channels
0 0.25 0.5 1
km

Figure 8

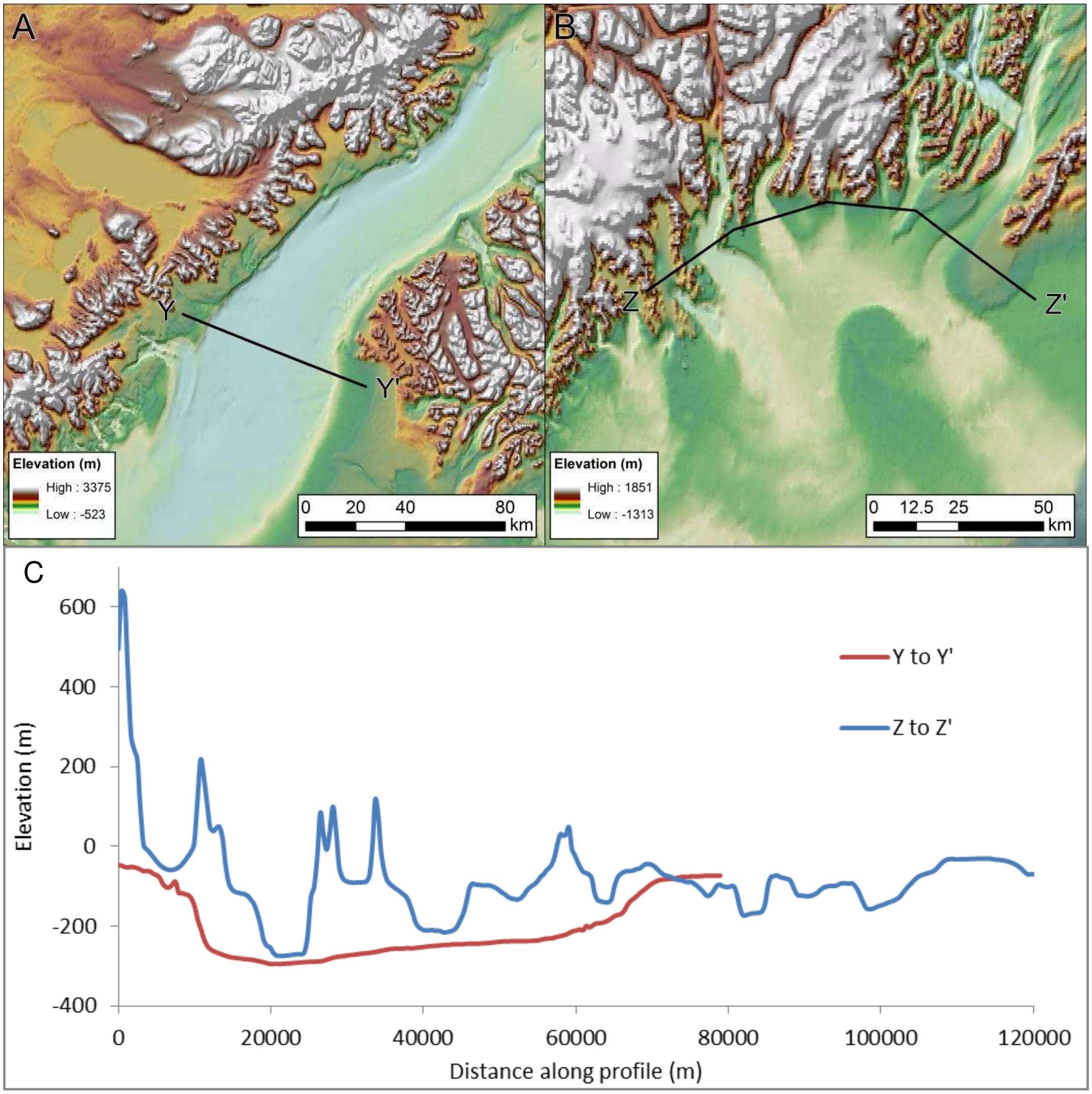
A
Y
Y'
Elevation (m)
High : 3375
Low : -523
0 20 40 80
km
B
Z
Z'
Elevation (m)
High : 1851
Low : -1313
0 12.5 25 50
km
C
Y to Y'
Z to Z'
Elevation (m)
600
400
200
0
-200
-400
0 20000 40000 60000 80000 100000 120000
Distance along profile (m)

Figure 9